We are IntechOpen,
the world's leading publisher of
Open Access books
Built by scientists, for scientists

6,900
Open access books available

185,000
International authors and editors

200M
Downloads

Our authors are among the

154
Countries delivered to

TOP 1%
most cited scientists

12.2%
Contributors from top 500 universities

BOOK CITATION INDEX
CLARIVATE ANALYTICS
INDEXED

WEB OF SCIENCE™

Selection of our books indexed in the Book Citation Index
in Web of Science™ Core Collection (BKCI)

Interested in publishing with us?
Contact book.department@intechopen.com

Numbers displayed above are based on latest data collected.
For more information visit www.intechopen.com

Nanofiltration Process Efficiency in Liquid Dyes Desalination

Petr Mikulášek and Jiří Cuhorka

Additional information is available at the end of the chapter

http://dx.doi.org/10.5772/50438

1. Introduction

Membrane science and technology has led to significant innovation in both processes and products over the last few decades, offering interesting opportunities in the design, rationalization, and optimization of innovative production processes. The most interesting development for industrial membrane technology depends on the capability to integrate various membrane operations in the same industrial cycle, with overall important benefits in product quality, plant compactness, environmental impact, and energetic aspects.

The membrane separation process known as nanofiltration is essentially a liquid phase one, because it separates a range of inorganic and organic substances from solution in a liquid – mainly, but by no means entirely, water. This is done by diffusion through a membrane, under pressure differentials that are considerable less than those for reverse osmosis, but still significantly greater than those for ultrafiltration. It was the development of a thin film composite membrane that gave the real impetus to nanofiltration as a recognised process, and its remarkable growth since then is largely because of its unique ability to separate and fractionate ionic and relatively low molecular weight organic species.

There are probably as many different applications in the whole chemical sector (including petrochemicals and pharmaceuticals) as in the rest of industry put together. Many more are still at the conceptual stage than are in plant use, but NF is a valuable contributor to the totality of the chemicals industry. The production of salt from natural brines uses NF as a purification process, while most chemical processes produce quite vicious wastes, from which valuable chemicals can usually be recovered by processes including NF. The high value of many of the products of the pharmaceutical and biotechnical sectors allows the use of NF in their purification processes [1,2].

Reactive dye is a class of highly coloured organic substances, primarily used for tinting textiles. The dyes contain a reactive group, either a haloheterocycle or an activated double bond, which, when applied to a fibre in an alkaline dye bath, forms a chemical bond between the molecule of dye and that of the fibre. The reactive dye therefore becomes a part of the fibre and is much less likely to be removed by washing than other dyestuffs that adhere through adsorption. Reactive dyeing, the most important method for the coloration of cellulosic fibres, currently represents about 20-30% of the total market share for dyes, because they are mainly used to dye cotton which accounts for about half of the world's fibre consumption.

Generally, reactive dyes are produced by chemical synthesis. Salt, small molecular weight intermediates and residual compounds are produced in the synthesis process. These salt and residual impurities must be removed before the reactive dyes are dried for sale as powder to meet product quality requirement. Conventionally, the reactive dye is precipitated from an aqueous solution using salt. The slurry is passed through a filter press, and the reactive dye is retained by a filter press. The purity of the final reactive dye product in conventional process is low, having a salt content around 30%. Furthermore, the conventional process is carried out in various batches, which makes the entire process highly labor intensive and causes inconsistency in the production quality.

In dye manufacture, like most other processes, there is a continual search for production methods that will improve product yield and reduce manufacturing costs. Dye desalting and purification, the process by which impurities are removed to improve the quality of the product, is currently one of the biggest applications for NF technology. Dye manufacturers are now actively pursuing the desalting of the finished dye prior to spray drying because it not only improves product quality, but makes spray drying more efficient because the granulation of the dye takes place without the production dust. NF is proving to be an ideal method for this salt removal [3,4].

Nanofiltration is the most recently developed pressure-driven membrane separation process and has properties that lie between those of ultrafiltration (UF) and reverse osmosis (RO). The nominal molecular weight cut-off (MWCO) of NF membranes is in the range 200-1000 Da. Separation may be due to solution diffusion, sieving effects, Donnan and dielectric effects. The rejection is low for salts with mono-valent anion and non-ionized organics with a molecular weight below 150 Da, but is high for salts with di- and multi-valent anions and organics with a molecular weight above 300 Da. Thus, NF can be used for the simultaneous removal of sodium chloride (salt) and the concentration of aqueous dye solutions [5,6].

Diafiltration is the process of washing dissolved species through the membrane, which is to improve the recovery of the material in permeate, or to enhance the purity of the retained stream. Typical applications can be found in the recovery of biochemical products from their fermentation broths. Furthermore, diafiltration can be found in removal of free hydrogel present in external solution to purification of a semi-solid liposome (SSL), purification of polymer nanoparticles, enhancing the protein lactose ratio in whey protein products, separating sugars or dyes from NaCl solution (desalting), and many other fields. According to the property of the solute and the selectivity of membrane, diafiltration can be used in the process of MF, UF or NF [7-12].

The aim of this study is also devoted to the mathematical modelling of nanofiltration and description of discontinuous diafiltration by periodically adding solvent at constant pressure difference.

The proposed mathematical model connects together the design equations and model of permeation through the membrane. The transport through the membrane depends on the different approaches. Firstly the membrane is regarded to a dense layer and in this case transport is based on solution-diffusion model [13,14]. Second approach is regarded membrane to porous medium. Models with this approach are based mainly on extended Nernst-Planck equation. Through this approach, a system containing any number of n ions can be described using set of (3n + 2) equations. In this approach, it is assumed that the flux of every ion through the membrane is induced by pressure, concentration and electrical potentials. These models describe the transport of ions in terms of an effective pore radius r_p (m), an effective membrane thickness/porosity ratio $\Delta x/A_k$ (m) and an effective membrane charge density X_d (mol/m^{-3}). Such a model requires many experiments for determination of these structural parameters. These models are hard to solve [6,7,12,15]. The last approach is based on irreversible thermodynamics. These models assume the membrane as "black box" and have been applied in predicting transport through NF membranes for binary systems (Kedem-Katchalsky, Spiegler-Kedem models). Perry and Linder extended the Spiegler and Kedem model to describe the salt rejection in the presence of organic ion. This model describes transport of ion through membrane in terms of salt permeability P_s, reflection coefficient σ [10,12,16-18]. In our work is solution-diffusion model used. The solution-diffusion model can be replaced by more theoretical model in future.

1.1. Theoretical model

Salt rejection of a single electrolyte has been described by Spiegler and Kedem [19] by the three transport coefficients: water permeability L_P, salt permeability P_S and reflection coefficient σ. For the curve describing salt rejection as a function of flow, the salt can be treated as a single electroneutral species.

Assuming linear local equations for volume and salt flows, these authors derived an expression of salt rejection R_S as a function of volume flux J_V. The local flux equations are:

$$J_V = -L_P\left(\frac{dp}{dx} - \sigma\frac{d\pi}{dx}\right) \tag{1}$$

$$J_S = -P\frac{dc_S}{dx} + (1-\sigma)c_S J_V \tag{2}$$

where salt rejection R_S is defined by the salt concentrations c_F and c_P in the feed and permeate streams respectively.

$$R_S = 1 - \frac{c_P}{c_F} \tag{3}$$

and

$$c_P = \frac{J_S}{J_V} \tag{4}$$

With constant fluxes, constant coefficients P and σ and with condition in Eq. (4), integration of Eq. (2) through the membrane thickness yields:

$$\frac{J_V(1-\sigma)\Delta x}{P} = \ln \frac{c_P \sigma}{c_P - c_F(1-\sigma)} \tag{5}$$

and then salt rejection can be expressed as:

$$R_S = \frac{(1-F)\sigma}{1-\sigma F} \tag{6}$$

where

$$F = e^{-J_V A}, \quad A = \frac{1-\sigma}{P}\Delta x = \frac{1-\sigma}{P_S} \tag{7}$$

where P is the local salt permeability and P_S is overall salt permeability.

In a mixture of electrolytes, the interactions between different ions can be very important and the behaviour of mixed solutions in NF cannot be predicted from the coefficients describing each salt separately. The differences in the permeabilities of ions lead to an electric field, which influences the velocity of each ion. Thus one needs to analyse all ion fluxes together. This analysis for the mixture of two electrolytes with common permeable counter ion and two co-ions, which are the rejected and the permeable ion respectively, is presented bellow.

1.2. Salt permeation in presence of retained organic ions

Consider a system (see Figure 1) which consists of semipermeable membrane separating two aqueous solutions with mixed electrolyte sharing a common permeable cation (*1*) and two anions which anion (*2*) is permeable through the membrane and anion (*3*) is fully rejected.

For the sake of simplicity let us consider a mixture of a mono-monovalent salt (*NaCl*) and a multifunctional organic anion C_x^{-v} containing v negatively charged groups per molecule in a sodium salt form.

The two electrolytes are fully dissociated as shown in Eq. (8).

$$NaCl \Leftrightarrow Na^+ + Cl^-$$
$$C_xNa_v \Leftrightarrow vNa^+ + C_x^{-v}$$

(8)

If we assume the salt as a single electroneutral species we can express the condition of equilibrium between feed and permeate solution as:

$$(a_1a_2)_F = (a_1a_2)_P$$

(9)

We can also consider the equilibrium between feed solution and the solution inside the membrane. Then the equilibrium condition can be expressed as:
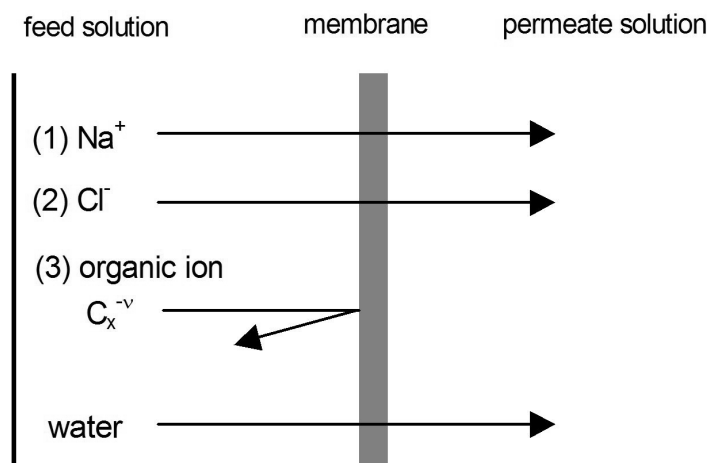
$$(a_1a_2)_F = (a_1a_2)_M$$

(10)

Figure 1. Scheme of the system.

In the feed solution containing a nonpermeable multifunctional organic anion at a concentration C_x, the following conditions of electroneutrality can be written for each phase:

$$[Cl^-]_F = c_{SF}$$

(11)

$$[X^-]_F = C_{xF}$$

(12)

$$[Na^+]_F = c_{SF} + vC_{xF}$$

(13)

$$[Cl^-]_M = [Na^+]_M = c_{SM}$$

(14)

We assume equilibrium on the membrane solution interface, approximating activities with concentrations and substituting Eqs. (11) and (14) into Eq. (10), one obtains the value of salt concentration inside the membrane on the feed side:

$$c_{SM} = c_{SF}\left(1 + \frac{vC_{xF}}{c_{SF}}\right)^{0.5} \tag{15}$$

The expression for c_{SM} from Eq. (15) is now used to integrate Eq. (5). In other words, in the presence of Donnan exclusion forces, induced by the impermeable organic ions, the salt transport across the membrane proceeds as if the membrane was exposed to a salt solution having a concentration c_{SM} instead of c_{SF}. Thus the value of c_{SM} and not of c_{SF} determines the driving force for the salt passage and should be used as boundary condition during the integration of Eq. (1) and Eq. (2).

Then the expression for salt rejection in the presence of retained organic ion can be written as:

$$R_S = \frac{(1-\sigma F)-(1-\sigma)\left(1 + \frac{vC_{xF}}{c_{SF}}\right)^{0.5}}{1-\sigma F} \tag{16}$$

1.3. Concentration dependence of the solute permeability

The concentration dependence of the solute permeability was proposed by Schirg and Widmer [16] as an exponential function:

$$P = \alpha c_F{}^\beta \tag{17}$$

where c_F is the concentration of the permeable component in the feed [g.l⁻¹],

α - coefficient for salt permeability [m.s⁻¹],

β - coefficient for concentration dependence of salt permeability [-].

With introducing of Eq. (17) into Eq. (6), the retention for single electrolyte can be written as:

$$R = 1 - \frac{1-\sigma}{1-\sigma\exp\left(\frac{(\sigma-1)J_V}{\alpha c_F{}^\beta}\right)} \tag{18}$$

Similar, with introduction of Eq. (17) into Eq. (16), the salt retention for the system with retained organic ion can be expressed as:

$$R_S = 1 - \frac{(1-\sigma_S)\left(1 + \frac{v M_S C_{xF}}{M_x c_{SF}}\right)^{0.5}}{1 - \sigma_S \exp\left(\frac{(\sigma_S - 1)J_V}{\alpha_S c_{SF}{}^{\beta_S}}\right)} \tag{19}$$

1.4. Mathematical modelling of diafiltration

Mathematical model connects together balance equations and solution-diffusion model, which is extended by dependence of salt permeability on the salt concentration in feed and Donnan equilibrium.

The balances for the concentration mode can be written as:

Solvent mass balance:

$$\frac{d(V_F \rho_F)}{d\tau} = -J A^* \rho_P \tag{20}$$

Mass balances of dye and salt:

$$\frac{d(V_F c_{D,F})}{d\tau} = -J A^* c_{D,P} \tag{21}$$

$$\frac{d(V_F c_{S,F})}{d\tau} = -J A^* c_{S,P} \tag{22}$$

Eq. (20) is possible to write in the form:

$$\frac{dV_F}{d\tau} = -J_V A^* \tag{23}$$

Mass balances of dye and salt are formally same and we can solve them together. Subscripts i represent dye and salt. Eq. (21) (or (22)), may be re-written as:

$$\frac{d(V_F c_{i,F})}{d\tau} = -J_V A^* (1 - R_i) c_{i,F} \tag{24}$$

where R_i is real rejection.

In the concentration mode, the volume and the concentration in feed depends on the time. Expanded differential equation with using the product rule can be written as:

$$V_F \frac{dc_{i,F}}{d\tau} + c_{i,F} \frac{dV_F}{d\tau} = -J_V A^* (1 - R_i) c_{i,F} \qquad (25)$$

Substituting Eq. (23) into Eq. (25) leads to:

$$V_F \frac{dc_{i,F}}{d\tau} = J_V A^* R_i c_{i,F} \qquad (26)$$

Dividing Eq. (26) by Eq. (23) leads to:

$$c_{i,F} = c_{i,F0} \left(\frac{V_{F0}}{V_F} \right)^{R_i} \qquad (27)$$

If we assume constant rejection and permeate flux (for small change of volume in feed tank, or better of yield - permeate volume divided by feed volume, it is achieved) or the average values integrations of Eq. (27) and Eq. (23) with the boundary conditions (V_{F0} to V_F) resulting in Eq. (28) and Eq. (29):

$$c_{i,F} = c_{i,F0} \left(\frac{V_{F0}}{V_F} \right)^{R_i} \qquad (28)$$

$$\tau = \frac{V_{R0} - V_R}{J_V A^*} \qquad (29)$$

On the base of Eq. (28) and Eq. (29) we can obtain the concentration in feed tank and the time for separation of certain permeate volume in concentration mode, respectively. Next process is diluting. Pure solvent (water) is used as diluant. Salt concentration in feed tank after this operation (c_S') is:

$$c_S' = c_{i,F0} \left(\frac{V_F}{V_{F0}} \right) \qquad (30)$$

This concentration (c_S') is now equal to the salt concentration in feed tank ($c_{S,F0}$) for the next concentration mode in the second diafiltration step.

For solving of these equations we need to know dependence of rejection and permeate flux on salt concentration in feed.

The basic equations for rejection can be written as:

$$J_S = B(c_F - c_P) \tag{31}$$

$$c_P = \frac{J_S}{J_V} \tag{32}$$

This model can be extended by the dependence of salt permeability on salt concentration in the feed [17]. To avoid some in conveniences with units, here c* is introduced and chosen to be 1 g/l.

$$B = \alpha \left(\frac{c_{S,F}}{c^*} \right)^\beta \tag{33}$$

Assuming equilibrium on the membrane - solution interface we can obtain (approximating activities with concentrations) [17]:

$$c_{S,W} = c_{S,F} \left(1 + \frac{v_D \cdot c_{D,F} \cdot M_S}{c_{S,F} \cdot M_D} \right) \tag{34}$$

In the presence of Donnan exclusion forces, induced by the impermeable organic ions, the salt transport across the membrane proceeds as if the membrane were exposed to a salt solution having concentration $c_{S,W}$ instead $c_{S,F}$. Thus the value of $c_{S,W}$ and not that of $c_{S,F}$ determines the driving force for the salt passage.

Then the expression for salt passage in the presence of retained organic ion can be written as:

$$J_S = \alpha \left(\frac{c_{S,F}}{c^*} \right)^\beta (c_{S,W} - c_{S,P}) \tag{35}$$

and then salt concentration in permeate can be expressed as

$$c_{S,P} = \frac{\alpha \dfrac{c_{S,F}^{\beta+1}}{c^{*\beta}} \left(1 + \dfrac{v_D \cdot c_{D,F} \cdot M_S}{c_{S,F} \cdot M_D} \right)}{J_V + \alpha c_{S,F}^\beta c^{*-\beta}} \tag{36}$$

For the permeate flux these equations can be used:

$$J_V = A(\Delta P - \Delta \pi_s - \delta) \tag{37}$$

Eq. (37) is the osmotic pressure model. This model is used in similar form by many authors [5,10,12-14,17,18]. Parameter A (water permeability) can be concentration or viscous de-

pended [12,14]. For our model we assume this parameter as constant. Coefficient δ represents the effect of dye on flux. This means mainly osmotic pressure of dye. If this parameter represents only osmotic pressure of dye, then it is constant too (constant dye concentration).

The osmotic pressure gradient for salt is related to the difference of the concentration Δc by the van´t Hoff law:

$$\Delta \pi_S = \frac{\nu R^* T}{M} \Delta c_S$$

(38)

where c is concentration,

A^* - membrane area,

A - water permeability,

B - salt permeability,

J - flux,

R - rejection,

R^* - universal gas constant,

M - relative molecular mass,

δ - coefficient for dye solution,

σ - reflection coefficient

ν - valence (for NaCl is $\nu = 2$ and for dye $\nu = 3$).

α - coefficient for salt permeability,

β - coefficient for concentration dependence of salt permeability

subscripts

$_S$ - salt

$_D$ - dye

$_V$ - water

$_F$ - feed

$_P$ - permeate

$_R$ - retentate

$_W$ - membrane interface (wall)

$_0$ - beginning of the concentration mode

1.5. Characterization of membranes

Before diafiltration experiments characterizations of commercial membranes are carried out. For these characterizations pure water and water solutions of salt are used. From experiments with pure water model parameter A (water permeability) can be estimated. This parameter is slope of the curve (straight line) J = f (ΔP) (see Eq. (37) and $\Delta\pi = \delta = 0$ because no salt and dye are used). In our model we assume water permeability as constant. However, an increase in concentration can cause significant changes in viscosity and a consequent modification of the water permeability. According to resistance model (A = 1/(μ R$_M$)) the dependence of water permeability on viscosity can be expressed as:

$$A_\mu = \frac{A}{\mu_{REL}}$$

(39)

where A is the water permeability respect to pure water and μ_{REL} is the relative viscosity of feed solution to pure water [12].

In case of diafiltration fouling or gel layer effects can occur and then parameter A is depended on dye/salt concentration ratio (in resistance model is added next resistance A=1/μ_{REL} (R$_M$ +R$_F$), where R$_M$ and R$_F$ are membrane and fouling resistance [14].

Similar experiments are made with salt solutions. Four salt concentrations (1, 5, 10 and 35 g/l) are used. From these experiments can be obtained parameter B (salt permeability) and then α and β (plotting B versus c$_F$). Values obtained from these experiments are not used direct but are used as first approximation values for best fit parameters (see Table 3). From results (salt rejection and flux) the suitable membranes for desalination were chosen, Desal 5DK, NF 70, NF 270 and TR 60. Membranes NF 90 and Esna 1 had higher rejection (see Figure 4). For desalination, than membrane with small rejection of salt are suitable.

1.6. Comparison of membranes

For comparison of membranes, three factors were used.

The first factor is separation factor of diafiltration, S:

$$S = \frac{\dfrac{c_D}{c_D^0}}{\dfrac{c_S}{c_S^0}} = \frac{c_D c_S^0}{c_D^0 c_S}$$

(40)

where c_D^0, c_S^0 are concentrations of dye and salt at the beginning of experiment, c_D, c_S are concentrations of dye and salt in the end of experiment.

The separation factor, S, represents how well the dye will be desalinated. With higher separation factor the dye desalination is better. But it is also clear that with bigger separation factor the loss of the dye will be bigger because real membranes have not 100% rejection of dye.

The dye loss factor, Z, can be defined as the rates of amount of the dye in permeate to amount of the dye at the beginning of experiment:

$$Z = \frac{V\left(c_D^0 - c_D\right)}{V c_D^0} = 1 - \frac{c_D}{c_D^0} \tag{41}$$

The third parameter is time of diafiltration needed to reach certain separation factor, S. The total time of diafiltration with n steps, τ, can be expressed (constant permeate flux in each concentration mode) as:

$$\tau_{total} = \sum_{i=1}^{n} \frac{\Delta V}{Q} = \sum_{i=1}^{n} \frac{V_{F0} - V_F}{AJ} \tag{42}$$

where Q is flow of permeate.

2. Methods

2.1. Membranes

Eight NF membranes were chosen for this study. Properties of membranes used are given in Table 1.

Indication	Type	Producer	MWCO [Da]	Material	Module
Desal 5DK	Desal 5DK	GEW & PT	200	polyamide	spiral-wound
Esna 1	Esna 1	Hydranautics	100-300	polyamide	spiral-wound
NF 270	NF 270	Dow	270	polyamide	spiral-wound
NF 90	NF 90	Dow	90	polyamide	spiral-wound
NF 70	CSM NE 2540-70	Saehan	250	polyamide	spiral-wound
NF 45	NF 45	FILMTEC	100	polyamide	spiral-wound
TR 60	TR 60 - 2540	Toray	400	polyamide	spiral-wound
PES 10	PES 10	Hoechst	500-1000	polyether-sulphone	spiral-wound

Table 1. Properties of the membranes used.

2.2. Materials

Dye was obtained from VÚOS a.s. Pardubice, Czech Republic. The commercial name is Reactive Orange 35, and a molecular weight is 748.2 Da in free acid form (three acidic groups) or 817.2 Da as the sodium salt. Figure 2 shows structural formula of the free acid form.

NaCl and MgSO$_4$ used for all experiments were analytical grade. The demineralised water with the conductivity between 4-15 µS/cm was used in this study.
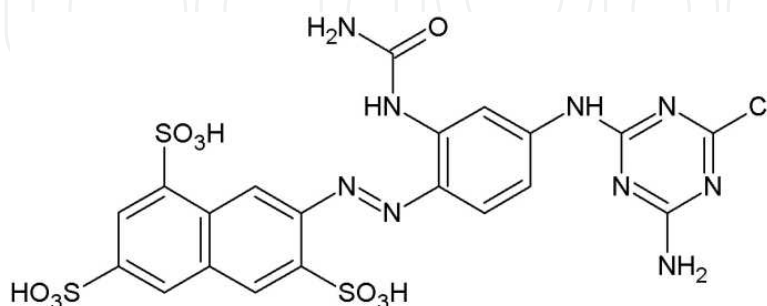

Figure 2. Structural formula of dye (free acid).

2.3. Experimental system

Experiments were carried out on system depicted schematically on Figure 3. Feed (F) was pumped by pump (3) (Wanner Engineering, Inc., type Hydracell G13) from feed vessel (2) to membrane module (1). Pressure was set by valve (4) placed behind membrane module. Permeate (P) and retentate (R) were brought back to feed vessel. Pressure was measured by manometer (5). Temperature was detected by thermometer (6). Stable temperature was maintained by cooling system (7).

2.4. Analytical methods

Dye concentrations were analysed using a spectrophotometer (SPECOL 11). NaCl and MgSO$_4$ concentrations were calculated from conductivity measurements using a conductivity meter (Cond 340i). Permeate and retentate salt concentrations during diafiltration experiments were analysed using potentiometric titration.

2.5. Separation procedure

The system was operated in the full recirculation mode while both retentate and permeate were continuously recirculated to the feed tank except sampling and concentration mode of diafiltration. By changing applied pressure (from 5 to 30 bar) and concentration of salt (1, 5, 10 and 35 g/l) in characterization of membranes both the retentate and permeate were returned back to the feed tank for 0.5 h or 10 min, respectively to reach a steady state before sampling. Before first concentration mode in diafiltraton experiments and after each diluting mode the total recirculation was used 1h and minimally 5 min, respectively. The permeate flux was measured by weighing of certain permeate volume and using a stopwatch.
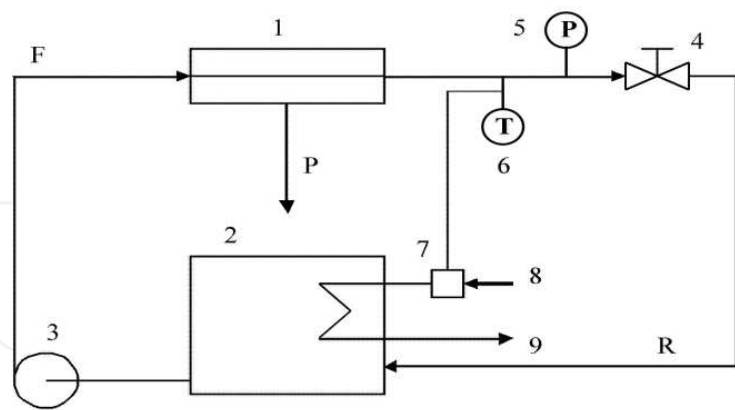
Figure 3. Schematic diagram of the experimental set-up used: 1 membrane module, 2 feed vessel, 3 high pressure pump, 4 back pressure valve, 5 manometer, 6 temperature controller, 7 cooling system, 8 cooling water input, 9 cooling water output, F feed, P permeate, R retentate (concentrate).

3. Results and discussions

3.1. Pure water flux

Water permeability is one of the basic characteristic of NF membranes. The pure water permeability of the eight membranes was determined by measuring the deionized water flux at different operating pressures. According to Darcy´s law, the permeate flux is directly proportional to the pressure difference across the membrane. The slope of this line corresponds to the water permeability (A).

Membrane	A [l/m².h.bar]
Desal 5DK	3.365
Esna 1	4.824
NF 90	5.845
NF 270	6.801
NF 70	2.650
NF 45	3.184
TR 60	3.952
PES 10	12.583

Table 2. Water permeability of membranes used.

As we can see the water permeability of PES 10 is approximately three times higher than water permeability of other membranes. It can be due to more open structure of this membrane, which can approach to the UF type. But the opened structure may cause the insufficient retention of the dye in the case of the dye-salt separation.

3.2. Flux and salt rejection in single salt solutions

Basic membrane characteristics are the dependence of the permeate flux and the salt rejection on other operation parameters, i.e. the applied pressure difference and the salt concentration in feed.

The permeate flux increases with increasing pressure and decreases as the feed concentration of salt increases. For the lowest concentration of salt (1 g/l), the values of permeate flux were similar to the values of clean water. The lower values of permeate flux were obtained with the increasing salt concentrations in feed (increasing osmotic pressure). For membrane NF 90 fluxes were not measured at the highest salt concentration for pressure smaller than 25 bar, because the osmotic pressure was too high. Opposite problem was with membrane NF 270 at the smallest salt concentration in feed. The permeate flux was too high and pump was not able to deliver necessary volumetric flow of retentate (600 l/h) for constant conditions at all experiments.

The observed rejection increases as the pressure difference increases, and decreases with the increasing salt concentration in feed for all tested membranes. However, the minimal values were obtained during experiments with membrane NF 270. Low values of the salt rejection and higher values of the permeate flux are suitable for desalting. Figure 4 shows the comparison of tested membranes for the lowest (1 g/l) and the highest salt concentrations in feed (35 g/l), respectively.
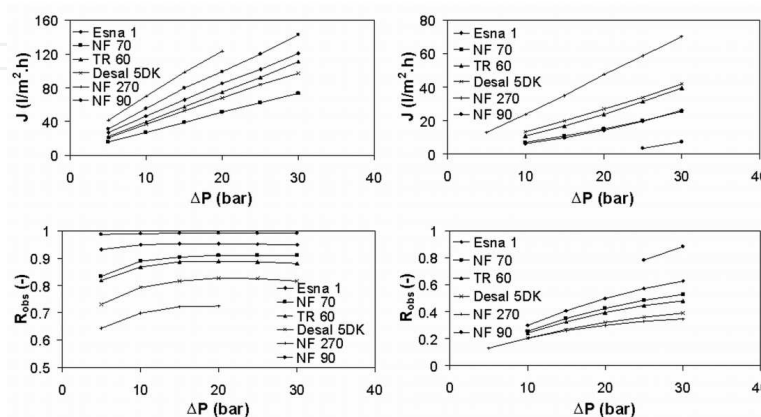

Figure 4. Permeate flux and rejection as a function of pressure for the lowest salt concentration; (1 g/l) - left figures and the highest salt concentration (35 g/l) - right figures.

Figure 5 denote dependence of the transmembrane pressure on the flux for NaCl solutions with the various salt contents. As we can see this dependence for every salt concentration shows a straight line course. Thus we can assume that the concentration polarization has no significant influence and therefore we can consider the bulk concentration equal to that on the membrane [20], which is required in model equations.
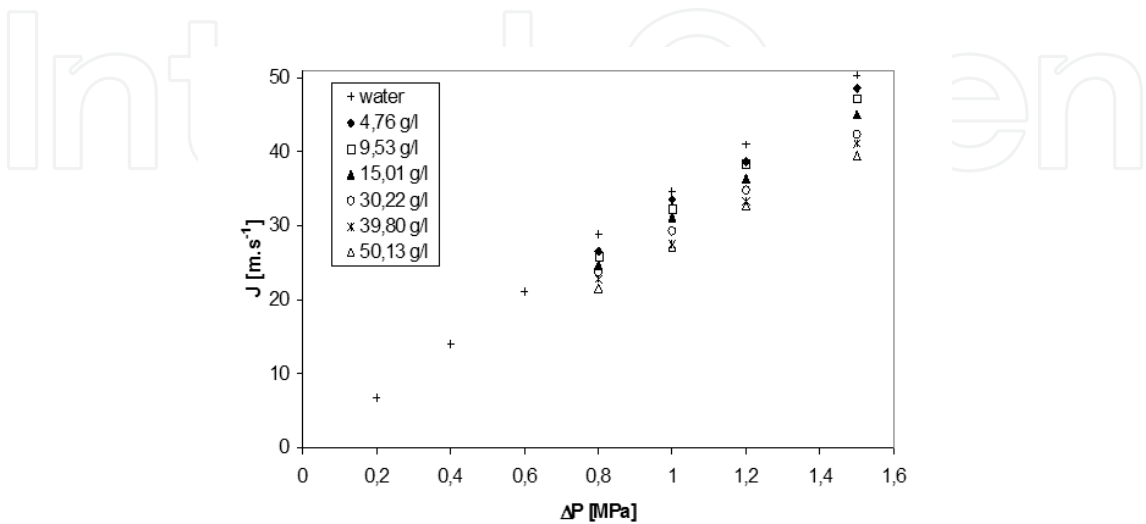

Figure 5. Flux as a function of transmembrane pressure for NaCl solutions with various salt content (Desal 5DK).

Experimental data rejection-flux can be evaluated by extended Spiegler-Kedem model to obtain parameters σ, α and β.

Membrane	L_P [m.s^{-1}.Pa^{-1}]	$\Box$ [-]	$\Box$ [m.s^{-1}]	$\Box$ [-]
Desal 5DK	$9.35.10^{-12}$	0.824	$1.96.10^{-6}$	0.438
Esna 1	$1.34.10^{-11}$	0.594	$1.60.10^{-6}$	0.620
NF 90	$1.62.10^{-11}$	0.685	$4.39.10^{-6}$	0.266
NF 270	$1.89.10^{-11}$	0.723	$2.88.10^{-6}$	0.529
NF 70	$7.36.10^{-12}$	0.598	$1.34.10^{-6}$	0.381
TR 60	$1.10.10^{-11}$	0.583	$1.86.10^{-6}$	0.474

Table 3. Coefficients of extended Spiegler-Kedem model for the transport of NaCl for various membranes.

The membrane PES 10 was not involved into Table 3 because this membrane didn't show typical course of the rejection-flux dependence. These differences are caused by another nature of this membrane near the UF type and therefore the transport through this membrane cannot be described by Spiegler-Kedem model.

On the Table 3 we can see that the water permeability and the salt permeability show the same trend for various membranes (L_P and α). The parameter σ means the maximum rejec-

tion attainable on given membrane (at the lowest concentration and the highest pressure). The parameter β express the concentration dependence of the salt permeability. The analyzation of experimental data for separation of $MgSO_4$ by Spiegler-Kedem model is less interesting because except PES 10 all membranes showed rejection almost equal unity.

3.3. Flux, salt and dye rejection in mixed dye - salt solutions

The aim of these experiments was to find dependence of salt and dye rejections on the salt and dye concentration. In every experiment carried out in this work the dye rejection was sufficient high and almost equal unity. The lowest value of the dye rejection observed was 0.9988. The salt rejection as a function of the dye and salt concentration is plotted in following Figure 6.

It can be seen from Figure 6 that the salt rejection decreases with decreasing salt concentration and with increasing dye concentration, corresponding to Donnan equilibrium (Eq. 15).

In the case of solution without the dye or with low dye content (positive rejections) we can observe the typical decline of salt rejection with increasing salt concentration. At higher dye content we can observe increase of salt rejection with increasing salt concentration due to shifting of Donnan equilibrium.

It's obvious from Figure 7 that salt content has also a strong influence on the flux. In the case of single salt solution (without dye content) we can see a typical decrease of flux with increasing salt content. In the case of mixed dye-salt solutions we can observe initial increase of flux and following decrease after a maximum was reached. The initial increase of flux at high dye concentration and low salt concentration is due to negative rejection (see Figure 6), which causes the reverse osmotic pressure difference between permeate and feed side of the membrane ($\Delta\pi>0$). This reverse osmosis pressure difference escalates the driving force of the process (Eq. 1) thus flux increases.

The experimental dependence of the salt rejection on flux can be evaluated by extended Spiegler-Kedem model (Figure 8) in order to obtained parameters σ_{NaCl}, α_{NaCl} and β_{NaCl}. These parameters are characteristic for the transport of NaCl through given membrane and also characteristic for given dye in feed solution dye. The meaning of individual parameters is the same as in the case of the single salt transport.

Figure 8 depicted the experimental dependence of the salt rejection on the flux. The single curves represent course of the salt rejection as a function of the flux for given dye content in the feed. The pressure difference was kept constant during all experiments and flux was changed by changing of salt content in the feed (changing of osmotic pressure difference).

It can be seen from Figure 8 that extended Spiegler-Kedem model isn't able to evaluate rejection-flux data as accurately as it was in the case of the single salt transport. But realising the range of rejection values we can consider prediction by this model still sufficient.

We can see that the coefficient α is approximately four times higher than in the case of the separation of single NaCl solution, which reflect the fact that the presence of the dye escalate the salt permeability through the membrane.
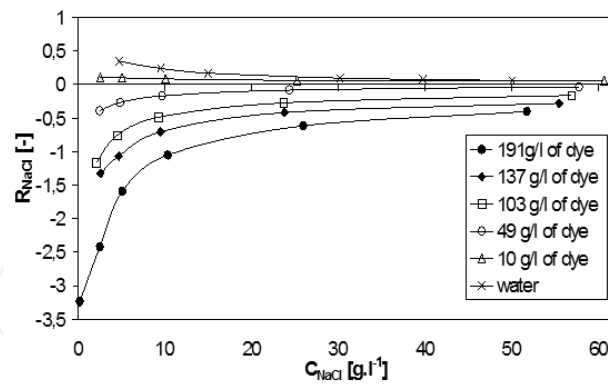
Figure 6. Salt rejection as a function of salt concentration for different dye concentration (Desal 5DK; 1.5MPa).
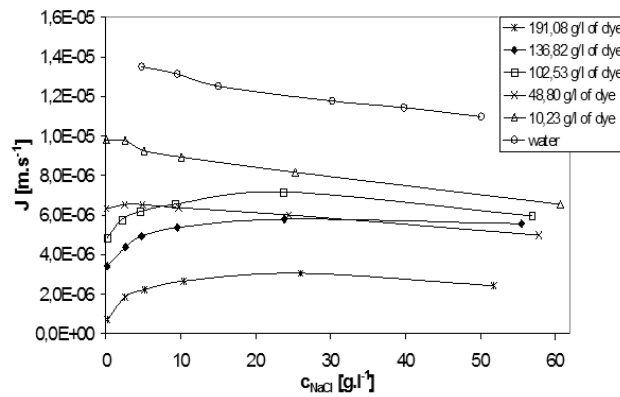

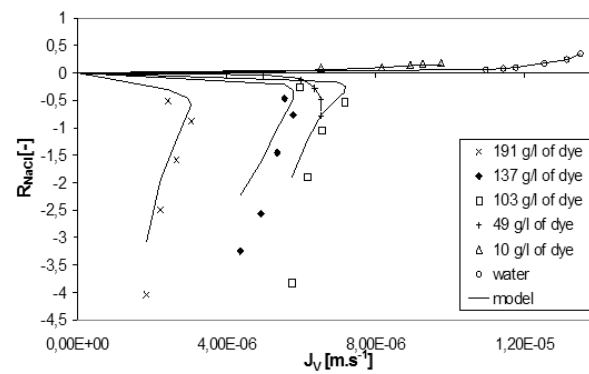**Figure 7.** Flux as a function of salt concentration for different dye concentration (Desal 5DK).

Figure 8. Salt rejection as a function of flux for different dye concentration (Desal 5DK; 1.5 MPa); $\sigma_{NaCl}=0.880$; $\alpha_{NaCl}=5.38.10^{-6}$ and $\beta_{NaCl}=0.623$.

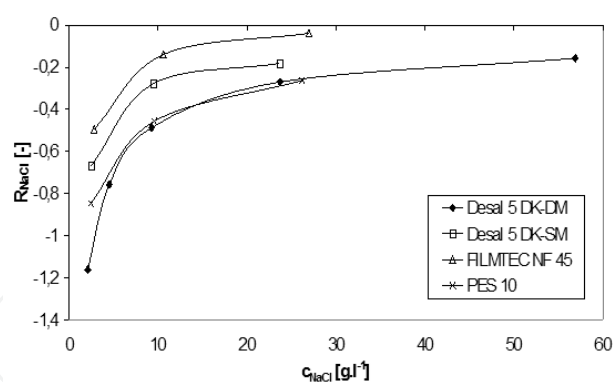**Figure 9.** Comparison of rejection-NaCl concentration dependence for various membranes at dye concentration 100 g.l^{-1} (1.5 MPa).

The comparison with another membranes was carried out in order to determine the most suitable one of given membranes. As we can see at Figure 9 membranes Desal 5DK and PES 10 have the best course of dependence of salt rejection as a function of concentration but PES 10 shows the highest flux (Figure 10). Among given membranes PES 10 is therefore the most suitable membrane for desalination of this dye.
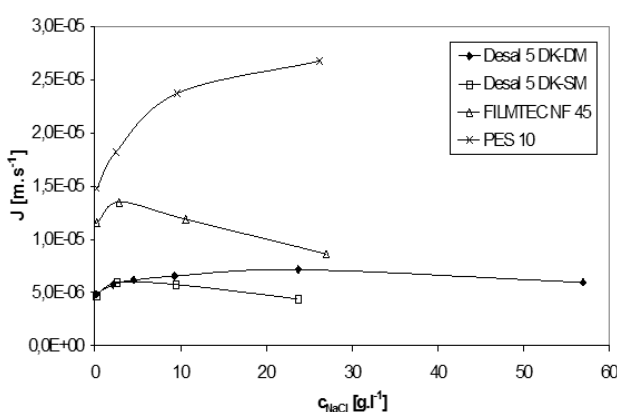

Figure 10. Comparison of flux-NaCl concentration dependence for various membranes at dye concentration 100 g.l^{-1} (1.5 MPa).

3.4. Diafiltration

The concentration of macrosolutes by batch NF is frequently accompanied by a diafiltration step to remove microsolutes such as salts. Batch diafiltration with periodically adding solvent at 20 bars and constant retentate flow 600 l/h was provided. Aqueous dye solutions with dye concentrations 100, 50 and 10 g/l and salt concentration between 20-23 g/l were desalted at 23 C. Volume of the pure solvent added in every dilute mode was 4l (the same volume of permeate was remove before in concentration mode). Total feed volume in tank was 52l. For every membrane and every concentration of the dye in feed fifty diafiltration steps were made. One point in Figures 11-14 is one diafiltration step before concentration mode.

Four membranes only - Desal 5DK, NF 70, NF 270 and TR 60 - were used for diafiltration experiments. Diafiltration with membrane NF 270 was provided only with dye concentrations 100 and 50 g/l and with membrane TR 60 only at the highest dye concentration, which is the best for desalination. For the reason of low values of permeate flux, membrane NF 90 and Esna 1 were not used for those experiments.

Dependences of rejection on salt concentration in feed are given in Figure 11 for Desal 5DK, NF 70, NF 270 and TR 60, respectively. Membranes are compared at dye concentration 100 g/l. The lowest values of rejection (max. 0.29) were obtained for membrane Desal 5DK. The membrane NF 70 had the highest values.

Dependences of flux on salt concentrations are shown in Figure 12. The highest values of flux (70.3 l/m².h) were obtained in experiments with membrane NF 270. The permeate flux decreased while salt concentration increased. This is due to the effect of osmotic pressure along with the concentration polarization. Due to the concentration polarization phenomenon, the osmotic pressure of the aqueous solution adjacent to the membrane active layer is higher than the corresponding value of the feed solution. As a result, the osmotic pressure would increase dramatically while the salt concentration increased.

In Figure 13 dependences of salt concentrations on time of diafiltration are shown.
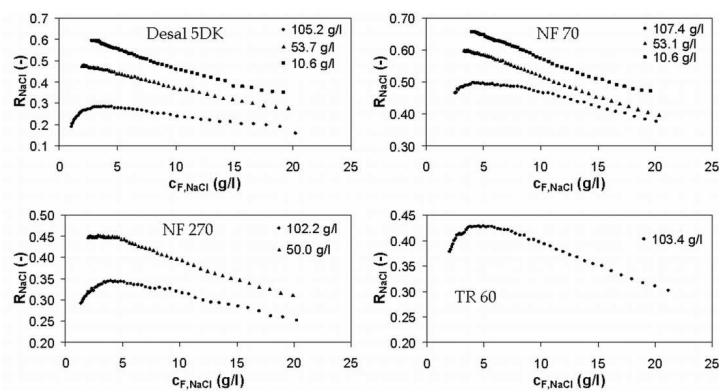

Figure 11. Salt rejection as a function of salt concentration in feed

Membrane	A [l/m².h.bar]	□ [l/m².h]	□ [-]	□ [bar]
Desal 5DK	3.365	5.379	0.623	7.503
NF 70	2.650	4.839	0.381	4.664
NF 270	6.801	10.350	0.529	8.561
TR 60	3.952	6.693	0.474	5.888

Table 4. Model parameters.

The comparisons of experimental and model data for the highest dye concentration (100 g/l) are shown in Figure 14. Salt concentrations are calculated using Eq. (28) and Eq. (30). Rejection needed for these equations is calculated on basis of Eq. (36). Best fit parameters for proposed model are given in Table 4.

From Table 4 can be shown that δ is not only osmotic pressure (if we assume water permeability as constant), because the values of δ are different. From these results we can assume, the highest effect of dye on flux is for membrane NF 270. This membrane is the most fouled from these membranes. It is appropriate assumed the change in water permeability (A) in case of desalination of dyes.

In our experiments, the decrease of permeate flux was mainly caused by the effect of concentration polarization and the increase of the viscosity of dye solution. The dye formed a boundary layer over the membrane surface (concentration polarization) and consequently, increased the resistance against the water flux through the membrane. At the same time, the viscosity of solution increased with higher concentration.

From Figure 14 can be shown that the experimental results in permeate fit the model very well. Due to considerably low salt concentrations in permeate, concentration polarization was minimized. The diafiltration process benefits to obtain pure salt product and this can be predicted by a mathematic model on the basis of description of discontinuous diafiltration by periodically adding solvent at constant pressure difference.
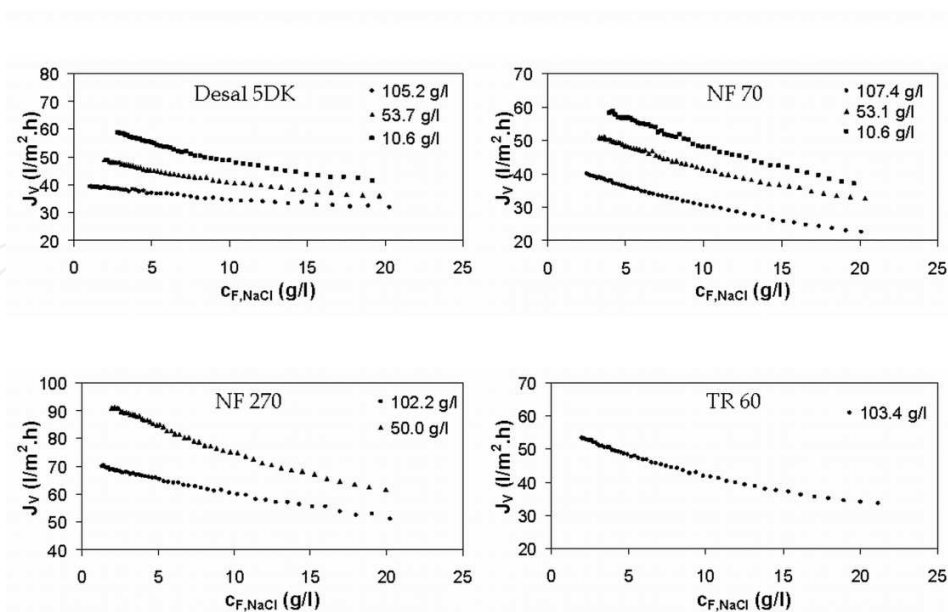

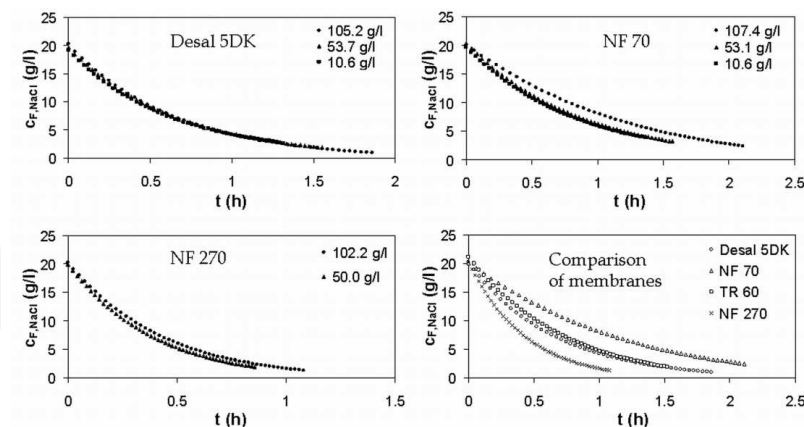**Figure 12.** Permeate flux as a function of salt concentration in feed.

Figure 13. Salt concentration as a function of diafiltration time for membranes Desal 5DK, NF 70, NF 270 and comparison of tested membranes at dye concentration 100 g/l.
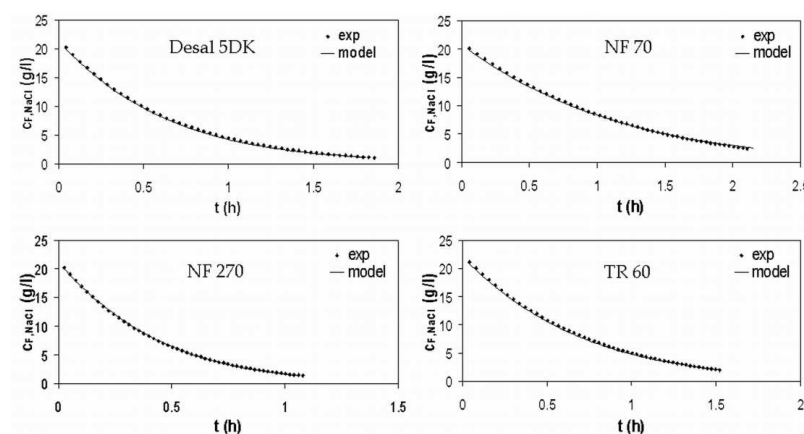

Figure 14. Comparison of experimental and model data for the highest dye concentration.

From Table 5 is clearly shown, the total time of diafiltration, τ_{total}, decreases with decreasing dye concentration. The shortest time had membrane NF 270. Time for the highest dye concentration is not two times higher than with medium dye concentration for all tested membranes (the time/amount of dye desalted ratio is the smaller for higher concentration of dye). Separation factor decreases with decreasing concentration of dye and it is the second reason why the highest dye concentration was used as the best mode for desalination. The best separation factor had membrane Desal 5DK (very similar values, except the highest dye concentration, had membrane NF 270). The loss of dye is almost same for membrane Desal 5DK, NF 70 and NF 270 at all concentrations of dye. Only for membrane TR 60 are obtained higher loss of dye.

DESAL 5DK				
$c_{F,NaCl,Z}$	(g/l)	22.00	19.62	19.21
$c_{F,NaCl,K}$	(g/l)	0.97	1.88	2.70
$c_{F,dye,Z}$	(g/l)	105.17	53.75	10.61
$c_{F,dye,K}$	(g/l)	105.15	53.74	10.60
τ_{total}	(hod)	1.86	1.55	1.32
S	(-)	22.71	10.44	7.10
Z	(%)	0.02	0.01	0.07
NF 70				
$c_{F,NaCl,Z}$	(g/l)	20.08	20.33	19.64
$c_{F,NaCl,K}$	(g/l)	2.40	3.21	3.86
$c_{F,dye,Z}$	(g/l)	107.42	53.05	10.56
$c_{F,dye,K}$	(g/l)	107.38	53.04	10.56
τ_{total}	(hod)	2.11	1.57	1.37
S	(-)	8.37	6.34	5.09
Z	(%)	0.03	0.03	0.05
TR 60				
$c_{F,NaCl,Z}$	(g/l)	21.14	20.56	19.72
$c_{F,NaCl,K}$	(g/l)	1.88	2.22	3.16
$c_{F,dye,Z}$	(g/l)	103.41	53.65	10.71
$c_{F,dye,K}$	(g/l)	102.74	53.16	10.52
τ_{total}	(hod)	1.52	1.25	0.98
S	(-)	11.17	8.98	6.25
Z	(%)	0.65	0.48	0.18
NF 270				
$c_{F,NaCl,Z}$	(g/l)	22.00	19.92	20.64
$c_{F,NaCl,K}$	(g/l)	1.28	1.90	2.68
$c_{F,dye,Z}$	(g/l)	102.15	49.98	10.52
$c_{F,dye,K}$	(g/l)	102.12	49.97	10.53
τ_{total}	(hod)	1.08	0.86	0.67
S	(-)	17.19	10.50	6.89
Z	(%)	0.03	0.04	0.04

Table 5. Total time of diafiltration, τ_{total}, the separation factor, **S**, and the loss of dye, **Z**. (subscript $_{Z,K}$ are start and end of diafiltration, respectively)

4. Conclusions

The separation performance of dye, salt and dye solution with six different nanofiltration membranes were investigated, followed by the study of the optimum of diafiltration and concentration process of dye solution.

Asymmetric and negatively charged polyamide thin-film composite membranes of near similar molecular weight cut-off were characterized for key physical and surface properties, and employed to perform the laboratory-scale experiments to investigate the impacts of membranes properties on reactive dye removal from dye/salt mixtures through NF process. It was found that properties of the NF membrane play an important role in dye removal rate, stable permeate flux and their change behaviour with operational conditions.

The electrostatic repulsive interaction between dye and membrane surface promotes the dye removal and decreases concentration polarization and dye adsorption on the membrane surface. But, the action will be weakened as the dye concentration or salt concentration increased.

The introduction of an exponential term for the concentration dependence of salt permeability in the Spiegler-Kedem model allows very good prediction of rejection of nanofiltration membranes for single salt solutions depending on the feed concentration and permeates flux.

In the case of separation of mixed dye-salt solutions the extended Spiegler-Kedem model including Donnan equilibrium term (the Perry-Linder model) and the exponential concentration dependence term can be used for sufficient prediction of the salt rejection even at high dye concentrations typical for industrial desalination process.

From the results presented above it is clear that the best concentration of the dye in feed for desalination of reactive dye by batch diafiltration is 100 g/l. In this case the salt rejection reaches minimal value due to Donnan potential which strengthens the flow of salt through the membrane.

The best membrane for desalination is NF 270 which has smaller dye loss factor and the shortest time of diafiltration. Very suitable membrane is also Desal 5DK, which has the best separation factor and dye loss factor, but this membrane has longer time of diafiltration (see Table 5). For desalination qualitative description it is convenient to use the proposed model.

Acknowledgements

Author details

Petr Mikulášek[*] and Jiří Cuhorka

*Address all correspondence to: petr.mikulasek@upce.cz

Institute of Environmental and Chemical Engineering, University of Pardubice, Pardubice, Czech Republic

References

[1] Drioli, E., Laganh, F., Criscuoli, A., & Barbieri, G. (1999). Integrated Membrane Operations in Desalination Processes. *Desalination*, 122(2-3), 141-145.

[2] Diawara, C. K. (2008). Nanofiltration Process Efficiency in Water Desalination. *Separation & Purification Reviews*, 37(3), 303-325.

[3] Yu, S., Gao, C., Su, H., & Liu, M. (2001). Nanofiltration used for Desalination and Concentration in Dye Production. *Desalination*, 140(1), 97-100.

[4] He, Y., Li, G. M., Zhao, J. F., & Su, H. X. (2007). Membrane Technology: Reactive Dyes and Cleaner Production. *Filtration & Separation*, 44(4), 22-24.

[5] Mulder, M. (2000). Basic Principles of Membrane Technology. 2nd Ed., Dordrecht, Kluwer Academic Publishers.

[6] Oatley, D. L., Cassey, B., Jones, P., & Bowen, W. R. (2005). Modelling the Performance of Membrane Nanofiltration - Recovery of high-value Product from a Process Waste Stream. *Chemical Engineering Science*, 60(7), 1953-1964.

[7] Bowen, W. R., & Mohammad, A. W. (1998). Diafiltration by Nanofiltration: Prediction and Optimization. *AIChE Journal*, 44(8), 1799-1812.

[8] Weselowska, K., Koter, S., & Bodzek, M. (2004). Modelling of Nanofiltration in Softening Water. *Desalination*, 162(1-3), 137-151.

[9] Foley, G. (2006). Water Usage in Variable Volume Diafiltration: Comparison with Ultrafiltration and Constant Volume Diafiltration. *Desalination*, 196(1-3), 160-163.

[10] Al-Zoubi, H., Hilal, N., Darwish, N. A., & Mohammed, A. W. (2007). Rejection and Modelling of Sulphate and Potassium Salts by Nanofiltration Membranes: Neural Network and Spiegler-Kedem Model. *Desalination*, 206(1-3), 42-60.

[11] Wang, L., Yang, G., Xing, W., & Xu, N. (2008). Mathematic Model of Yield for Diafiltration. *Separation and Purification Technology*, 59(2), 206-213.

[12] Kovács, Z., Discacciati, M., & Samhaber, W. (2009). Modelling of Batch and Semibatch Membrane Filtration Processes. *Journal of Membrane Science*, 327(1-2), 164-173.

[13] Das, Ch., Dasgupta, S., & De , S. (2008). Steady-state Modelling for Membrane Separation of Pretreated Soaking Effluent under Cross Flow Mode. *Environmental Progress*, 27(3), 346-352.

[14] Cséfalvay, E., Pauer, V., & Mizsey, P. (2009). Recovery of Copper from Process Waters by Nanofiltration and Reverse Osmosis. *Desalination*, 240(1-3), 132-146.

[15] Hussain, A. A., Nataraj, S. K., Abashar, M. E. E., Al-Mutaz, I. S., & Aminabhavi, T. M. (2008). Prediction of Physical Properties of Nanofiltration Membranes using Experiment and Theoretical Models. *Journal of Membrane Science*, 310(1-2), 321-336.

[16] Schirg, P., & Widmer, F. (1992). Characterisation of Nanofiltration Membranes for the Separation of Aqueous Dye-salt Solution. *Desalination*, 89(1), 89-107.

[17] Koyuncu, I., & Topacik, D. (2002). Effect of Organic Ion on the Separation of Salts by Nanofiltration Membranes. *Journal of Membrane Science*, 195(2), 247-263.

[18] Kovács, Z., Discacciati, M., & Samhaber, W. (2009). Modelling of Amino Acid Nanofiltration by Irreversible Thermodynamics. *Journal of Membrane Science*, 332(1-2), 38-49.

[19] Spiegler, K. S., & Kedem, O. (1966). Thermodynamics of Hyperfiltration (Reverse Osmosis): Criteria for Efficient Membranes. *Desalination*, 1(4), 311-326.

[20] Xu, Y., & Lebrun, R. E. (1999). Comparison of Nanofiltration Properties of Two Membranes using Electrolyte and Non-electrolyte Solutes. *Desalination*, 122(1), 95-105.